# The Vav binding site of the non–receptor tyrosine kinase Syk at Tyr 348 is critical for $\beta_2$ integrin (CD11/CD18)–mediated neutrophil migration

Jurgen Schymeinsky, Anca Sindrilaru, David Frommhold, Markus Sperandio, Ronald Gerstl, Cornelia Then, Attila Mócsai, Karin Scharffetter-Kochanek, and Barbara Walzog

**Leukocyte adhesion via $\beta_2$ integrins (CD11/CD18) activates the tyrosine kinase Syk. We found that Syk was enriched at the lamellipodium during N-formyl-Met-Leu-Phe–induced migration of neutrophil-like differentiated HL-60 cells. Here, Syk colocalized with Vav, a guanine nucleotide exchange factor for Rac and Cdc42. The enrichment of Syk at the lamellipodium and its colocalization with Vav were absent upon expression of a Syk kinase-dead mutant (Syk K402R) or a Syk mutant lacking the binding site of Vav (Syk Y348F). Live cell imaging revealed that both mutations resulted in excessive lamellipodium formation and severely compromised migration compared with control cells. Similar results were obtained upon down-regulation of Syk by RNA interference (RNAi) technique as well as in Syk$^{-/-}$ neutrophils from wild-type mice reconstituted with Syk$^{-/-}$ bone marrow. A pivotal role of Syk in vivo was demonstrated in the Arthus reaction, where neutrophil extravasation, edema formation, and hemorrhage were profoundly diminished in Syk$^{-/-}$ bone marrow chimeras compared with those in control animals. In the inflamed cremaster muscle, Syk$^{-/-}$ neutrophils revealed a defect in adhesion and migration. These findings indicate that Syk is critical for $\beta_2$ integrin–mediated neutrophil migration in vitro and plays a fundamental role in neutrophil recruitment during the inflammatory response in vivo. (Blood. 2006; 108:3919-3927)**



## Introduction

Polymorphonuclear neutrophils (PMNs) play an important role in host defense and inflammation. During the acute inflammatory response, PMNs extravasate from the blood into the tissue, where they migrate toward the sites of lesion by following a gradient of chemoattractants.[1,2] Site-directed migration (chemotaxis) requires 3 different processes[3]: (1) the periodical formation of lamellipodia; (2) the establishment of cell polarity that is characterized by the formation of a posterior pole (uropod) and an anterior pole (leading edge) that forms the lamellipodium with enhanced sensitivity for chemoattractants; and (3) the translation of the external chemotactic gradient into an internal signaling gradient. This process of directional sensing is due to an asymmetric distribution of signaling components within the cell.[3] Accordingly, neutrophil-like differentiated HL-60 (dHL-60) cells, an established model for PMNs, orient their polarity in response to a chemoattractant gradient and perform site-directed migration.[4] Chemoattractants signal via G-protein–coupled receptors that are responsible for directional sensing and the establishment of the polarized sensitivity within the cell.[3] However, ordered leukocyte polarization not only requires the presence of chemoattractants, but also depends on adhesive cell–matrix interactions that are mediated mainly by the leukocyte adhesion molecules of the integrin family.[5] $\beta_2$ integrins (CD11/CD18) especially are critically involved in firm adhesion and migration of PMNs.[6]

Recently, we and others have shown that the non–receptor tyrosine kinase Syk is constitutively associated with CD18, the $\beta$ subunit of the $\beta_2$ integrins in human PMNs and in HL-60 cells.[7-9] Syk is widely expressed in hematopoietic cells and fulfills essential roles in hematopoietic cell functions like Fc receptor[10] and cytokine receptor signaling,[11] phagocytosis,[12] lymphocyte development,[13,14] and platelet activation.[15,16] Syk and ZAP-70, the other member of this protein family, contain 2 Src homology 2 (SH2) domains in a tandem repeat that are separated by the interdomain A. The C-terminal kinase domain is separated from the 2 SH2 domains by the interdomain B.[17] Outside-in signaling of Mac-1 (CD11b/CD18), the most abundant $\beta_2$ integrin on PMNs, occurs upon ligand binding to immobilized fibrinogen or the intercellular adhesion molecules–1 and –2.[18] Mac-1–mediated adhesion induces tyrosine phosphorylation of different signaling components, including Syk.[7] A physiologic role for Syk has been demonstrated previously for multiple $\beta_2$ integrin–mediated functions of murine PMNs, including the respiratory burst, degranulation, and spreading.[19] Recently, we have shown that endogenous Syk is enriched at the leading edge of both murine PMNs and HL-60 cells, where Syk plays a role in the stabilization of the leading edge of the polarized cell and colocalizes with CD18.[19,20] Syk has several downstream targets, including Hip-55, SLP-76, Pyk2, and Vav.[17,21] Vav is a guanine exchange factor for the Rho family GTPases Rac and Cdc42, which are both critical for the control of the actin cytoskeleton during leukocyte polarization and migration.[22,23] Recently, it has been shown that Vav plays a role in migration of human lymphocytes and murine macrophages.[24,25]

In this study, we analyzed the Syk signaling pathway underlying the control of lamellipodia formation and polarization of leukocytes migrating on immobilized fibrinogen, a native ligand of the $\beta_2$ integrin Mac-1.[18] We used dHL-60 cells transiently transfected

From the Department of Physiology, Ludwig-Maximilians-University Munich, Germany; Department of Dermatology and Allergic Diseases, University of Ulm, Germany; Department of Pediatrics, Neonatal Unit, University of Heidelberg, Germany; and the Department of Physiology, Semmelweis University School of Medicine, Budapest, Hungary.

Submitted December 22, 2005; accepted July 12, 2006. Prepublished online as *Blood* First Edition Paper, August 1, 2006; DOI 10.1182/blood-2005-12-030387.

The online version of this article contains a data supplement.

The publication costs of this article were defrayed in part by page charge payment. Therefore, and solely to indicate this fact, this article is hereby marked "advertisement" in accordance with 18 USC section 1734.

with cDNA constructs for wild-type Syk, a kinase-dead mutant of Syk (Syk K402R), or a Syk mutant lacking the Vav binding site (Syk Y348F) tagged with enhanced green fluorescence protein (EGFP) to study the molecular mechanisms of Syk-mediated control of leukocyte polarization and migration. The biological relevance of our findings was studied in vitro using murine $Syk^{-/-}$ PMNs obtained from wild-type mice reconstituted with $Syk^{-/-}$ bone marrow as well as in vivo using the reverse-passive Arthus reaction and the inflamed cremaster muscle as models for the acute inflammatory response.

## Materials and methods

### Materials

Bovine serum albumin (BSA), human fibrinogen, N-formyl-Met-Leu-Phe (fMLP), Percoll, polybrene, Ponceau S, tumor necrosis factor α (TNFα), and Tween-20 were obtained from Sigma (Deisenhofen, Germany). Piceatannol, PP2, and PP3 were obtained from Calbiochem (La Jolla, CA). KC was obtained from R&D Systems (Wiesbaden, Germany). Fibronectin, RPMI 1640 medium, fetal calf serum (FCS), penicillin, streptomycin, and phosphate-buffered saline (PBS) were obtained from Biochrom (Berlin, Germany). Iscove modified Dulbecco medium (IMDM), including L-glutamine and 25 mM HEPES and high-glucose Dulbecco modified Eagle medium (DMEM) with GlutaMAX I and pyruvate were purchased from Gibco (Karlsruhe, Germany). G418 was obtained from Applichem (Darmstadt, Germany).

### cDNA contructs

The human Syk cDNA clone (clone ID IRALp962E102Q2) was obtained from the German Genomic Resource Center (RZPD; Berlin, Germany). The coding region of Syk was cloned in the *Eco*RI/*Kpn*I site of the EGFP-C1 expression vector (BD Biosciences Clontech, New York, NY) using the following PCR primers: 5′-ATCGAATTCGAAGCATGGCCAGCAGC-3′, and 5′-CTGTGATCAAAGGCAGCCACTGGTACCG-3′. The EGFP-tagged Syk K402R and Syk Y348F mutants were obtained from the nonmutated EGFP-Syk plasmid by site-directed mutagenesis with the QuickChange mutagenesis kit (Stratagene, La Jolla, CA) using following primer sets: 5′-GAAAACCGTGGCTGTGAGAATACTGAAAAACGAGGC-3′ and 5′-GCCTCGTTTTTCAGTATTCTCACAGCCACGGTTTTC-3′ for EGFP-tagged Syk K402R; and 5′-TGGACACAGAGGGTCGAGAGCCCCTACGC-3′ and 5′-GCGTAGGGGCTCTCGAACACCTCTGTGTCCA-3′ for EGFP-tagged Syk Y348F. The introduction of the expected mutation was confirmed by automated DNA sequencing (Medigenomix, Martinsried, Germany). The EGFP–β-actin expression vector was a generous gift from Beat Imhof (Department of Pathology, Centre Medical Universitaire, Geneva, Switzerland).

### Animals and generation of bone marrow chimeras

$CD18^{-/-}$ homozygotes[26] and $CD18^{+/+}$ wild-type control mice were derived from heterozygote crosses on a mixed 129Sv × C57BL/6 background. Animals were maintained under specific pathogen–free conditions. Mice carrying the $Syk^{tm1Tyb}$ (referred to as $Syk^{-}$) mutation[14] were maintained as $Syk^{+/-}$ heterozygotes on the C57BL/6 genetic background. The generation of mice with a $Syk^{-/-}$ hematopoietic system was performed as described previously.[19] Animal experiments were institutionally approved.

### Cell culture and electroporation of dHL-60 cells

The human myeloid HL-60 cells (ACC 3) and the murine WEHI-3B cells (ACC 26) were obtained from the German Resource Centre for Biological Material (Braunschweig, Germany). Cell culture and neutrophil-like differentiation of HL-60 cells were performed as described.[20,23] For pharmacologic inhibition of Syk, cells were treated with 30 μM piceatannol or vehicle for control (DMSO). For inhibition of Src-family kinases, cells were treated with 10 μM PP2 or its inactive analog PP3.

For electroporation, a 400-μL aliquot of dHL-60 ($2 \times 10^7$ cells/mL) in IMDM was transferred to a Gene Pulser cuvette with an 0.4-cm electrode (Bio-Rad, Hercules, CA) and mixed with 30 μg endotoxin-free vector DNA. Cells were incubated for 10 minutes at room temperature (RT) and subjected to an electroporation pulse of 290 V and 1050 μF (EasyJect $T^+$ electroporator; Equibio, Kent, United Kingdom).

### Isolation of bone marrow neutrophils

Murine bone marrow PMNs were isolated from femurs and tibias and subsequently loaded on top of a discontinuous Percoll gradient (52%/64%/72%) and centrifuged at 1000*g* for 30 minutes. PMNs were harvested from the 64%/72% interface, washed in PBS, and cultivated for 24 hours in RPMI 1640 medium supplemented with 20% WEHI-3B–conditioned medium. PMN viability was greater than 95% as assessed by the trypan blue exclusion test, and purity was greater than 98% as analyzed by microscopy using Hemacolor staining (Merck, Darmstadt, Germany).

### Generation of stable HL-60 siRNA clones

For construction of the retroviral vector expressing a Syk-specific 21-bp head-to-head hairpin RNA (pSyk-Retro), 2 complementary DNA fragments were synthesized (Biomers.net, Ulm, Germany), annealed, and cloned into the *Sal*I and *Xba*I cloning sites of the retroviral pSuppressorRetro vector (Imgenex, San Diego, CA). The sequence used was described elsewhere.[27] Hek-293T cells were triple transfected with the pSyk-Retro vector (10 μg), pMDtet.G (10 μg), and pMD.gagpol (10 μg) as described.[28] For retroviral transduction, HL-60 cells ($2.5 \times 10^5$ cells/mL) were cocultured with transfected Hek-293T cells for 1 day in medium containing 8 μg/mL polybrene. HL-60 cells stably expressing the pSyk-Retro vector were selected by adding 1 mg/mL G418 into the growth medium for 2 weeks. Syk protein expression was measured by the Western blotting technique using the mouse anti–human Syk monoclonal antibody (mAb) and a polyclonal goat β-actin antibody (sc-1616; Santa Cruz Biotechnology, Santa Cruz, CA) for control. Down-regulation of Syk by the inserted small interfering RNA (siRNA) construct was observed for a period of approximately 2 weeks.

### Adhesion and migration assay

Cells ($1 \times 10^5$–$2 \times 10^5$) suspended in adhesion medium (PBS supplemented with 0.25% BSA, 0.1% glucose, 1.2 mM $Ca^{2+}$, and 1 mM $Mg^{2+}$) were plated onto fibrinogen or fibronectin (250 μg/mL)–coated coverslips (Saur, Reutlingen, Germany) and incubated for 5 minutes at 37°C. Upon stimulation of cells as indicated, time-lapse video microscopy was performed using a Zeiss 200M microscope equipped with a Plan-Apochromat 20×/0.75 numerical aperture (NA) objective (Figure 5C) or a Plan-Apochromat 63×/1.4 NA oil objective (Zeiss, Göttingen, Germany) (Figures 3, 4, and 5B), an AxioCam HR digital camera (Zeiss, Göttingen, Germany), and AxioVision 4 software (Zeiss, Munich-Hallbergmoos, Germany). Photoshop 7 software (Adobe Systems, San Jose, CA) was used to create panels of the recorded images. The quantitative analysis of the lamellipodium formation and the subcellular distribution of Syk and Vav were performed by 2 different investigators in a blinded manner using confocal images.

Migration of dHL-60 cells was studied in IBIDI μ-slides (IBIDI, Munich, Germany) coated with fibrinogen (250 μg/mL),[20] and the migration of murine PMNs was analyzed in Zigmond chambers.[29] Time-lapse video microscopy of cell migration was performed as described in the previous paragraph. Analysis of migration tracks was carried out using ImageJ version 1.33 provided by the National Institutes of Health (http://rsb.info.nih.gov/ij/) and the manual tracking plugin (written by Fabrice P. Cordelières, Institute Curie, Orsay, France). The migration tracks were plotted using SigmaPlot 8.0 Software (SPSS, Chicago, IL).

### Fluorescence staining and confocal microscopy

Cells were fixed with 3.7% formaldehyde in PBS for 30 minutes at 4°C and subsequently permeabilized using 0.2% Tween in PBS for 2 minutes, and

washed and blocked with 1% BSA in PBS at 4°C overnight. Syk was stained with a monoclonal mouse anti–human Syk antibody (clone 4D10; immunoglobulin $G_{2a}$ [$IgG_{2a}$]) or a polyclonal rabbit antibody directed against human and murine Syk (N-19; sc-1077) from Santa Cruz Biotechnology. Vav-1 was assessed using a polyclonal rabbit anti–human Vav antibody (Upstate Biotechnology, New York, NY). Alexa 546– or Alexa 488–conjugated secondary antibodies were used (Molecular Probes, Eugene, OR). F-actin was stained with Alexa 488– or Alexa 633–conjugated phalloidin (Molecular Probes). Confocal microscopy was performed using a Zeiss 63×/1.2 NA water differential interference contrast (DIC) objective (Figures 1, 2, and 5A) and an LSM 410/Axiovert 135 M microscope (Zeiss, Oberkochen, Germany).

### Arthus reaction

The cutaneous reverse-passive Arthus reaction was elicited by injecting BSA (2.5 mg/200 μL) intraperitoneally and 20 μL rabbit anti-BSA antibody (Sigma, Deisenhofen, Germany) subcutaneously in the left ear. Edema was measured by determining the ear thickness with a spring-loaded Oditest caliper (Kroeplin, Schüchtern, Germany) at 6 hours after induction of the Arthus reaction. Untreated contralateral ears served as controls. Specific edema formation was assessed by subtracting the thickness of the control ear from that of the challenged ear. The extent of hemorrhage was measured semiquantitatively as described previously.[30] For analysis of PMN extravasation, histologic sections were stained for Gr-$1^+$ cells as described.[31] Images were acquired using a Zeiss Axiophot microscope (Zeiss, Oberkochen, Germany) with an Axiocam color camera and corresponding software (Zeiss, Oberkochen, Germany). PMN extravasation was quantified by counting Gr-$1^+$ cells in 5 different microscopic fields.

### Whole-mount preparation of the cremaster muscle

Mice were anesthesized as described and placed on a heating pad to maintain body temperature.[32] Mouse cremaster muscles were surgically prepared as previously reported[32] and superfused with 1 μM fMLP in superfusion buffer for 15 minutes. To differentially count intravascular and extravascular leukocytes after fMLP superfusion, cremaster muscle whole mounts were prepared as described.[32] Fixed cremaster muscles were stained with Giemsa and analyzed using a Olympus microscope (BX51WI; Olympus, Hamburg, Germany) with a 60×/0.9 NA water objective (Olympus). Intravascular and interstitial leukocytes were counted and differentiated into neutrophils and mononuclear cells (Figure 7).

### Statistical analysis

Data shown represent means ± SD unless indicated otherwise. Statistical significance was determined using the Student *t* test. Statistical analysis of the in vivo data was performed using the Sigma-Stat 2.0 software package (SPSS). Leukocyte counts and differentials were compared with Student *t* test or by the Wilcoxon rank-sum test as appropriate. *P* values less than .05 were considered statistically significant.

## Results

### Generation of EGFP-Syk transfectants

In the present study, we generated different EGFP-tagged Syk constructs to unravel the molecular mechanism of Syk-mediated control of lamellipodium formation and migration. dHL-60 cells were stimulated with 100 nM fMLP to induce $\beta_2$ integrin–dependent cell adhesion and polarization on immobilized fibrinogen. Similar to untransfected dHL-60 cells, in which Syk was enriched at the leading edge of the polarized cell as detected by Syk antibody staining, the EGFP-Syk wild-type transfectants revealed a bipolar phenotype that was characterized by an enrichment of Syk at the lamellipodium where Syk colocalized with F-actin (Figure 1A). According to this, the EGFP-actin transfectants underwent a shape change and established a bipolar phenotype upon stimulation. Again, the lamellipodium was characterized by the enrichment of F-actin and endogenous Syk as detected by Syk antibody staining. Thus, the transfectants were functional and showed similar characteristics compared with the nontransfected wild-type

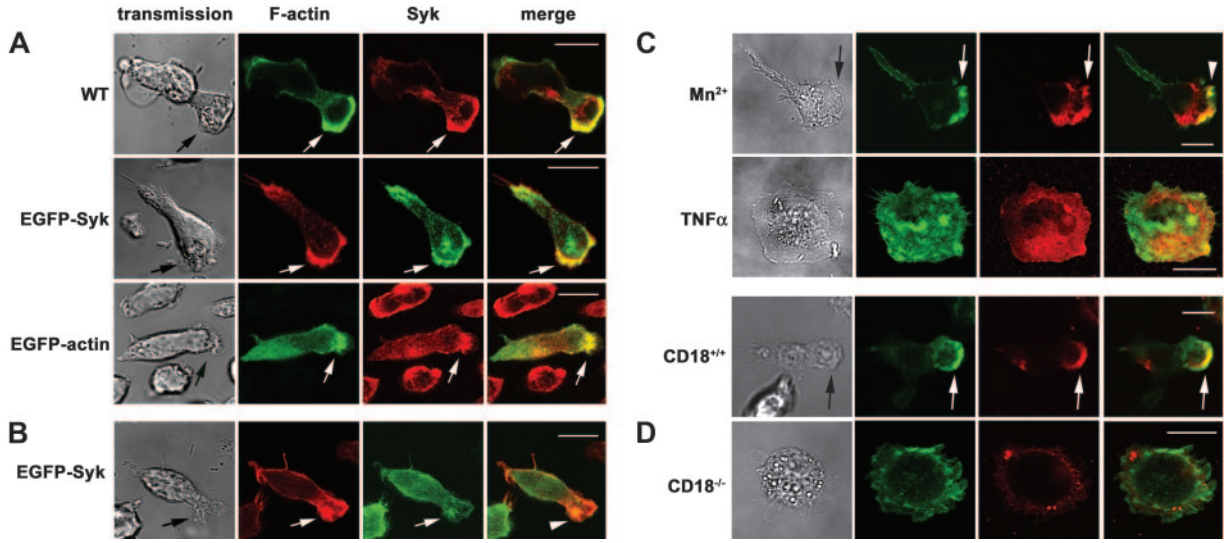


**Figure 1. Syk was enriched at the leading edge upon $\beta_2$ integrin–mediated adhesion.** Confocal microscopy images of human Syk detected by a mouse anti–human Syk mAb and a secondary Alexa 546–conjugated anti–mouse IgG Ab (red) or Syk-EGFP epifluorescence (green). Murine Syk was detected using a rabbit anti–mouse Syk Ab and an Alexa 546–conjugated anti–rabbit IgG Ab (red). F-actin was assessed using Alexa 488–conjugated phalloidin (green), EGFP-actin epifluorescence (green), or Alexa 633–conjugated phalloidin (red). (A) Upon induction of adhesion of untransfected dHL-60 cells (WT), EGFP-Syk– or EGFP-actin–transfected dHL-60 cells by fMLP (100 nM) on immobilized fibrinogen, F-actin and Syk were enriched at the leading edge (arrow). The merged images demonstrate colocalization (arrow, yellow). (B) Upon induction of adhesion of EGFP-Syk–transfected dHL-60 cells by fMLP (100 nM) on immobilized fibronectin, the enrichment of Syk at the leading edge was absent (arrowhead). (C) Upon induction of adhesion of untransfected dHL-60 cells by $Mn^{2+}$ (0.2 mM) on immobilized fibrinogen, Syk was enriched at the leading edge (arrow), whereas TNFα (30 ng/mL) induced cell spreading without an obvious formation of a leading edge. (D) Upon induction of adhesion of murine $CD18^{+/+}$ PMNs on immobilized fibrinogen by fMLP (100 nM), Syk was enriched at the leading edge (arrow), whereas Syk was homogenously distributed in $CD18^{-/-}$ PMNs, which showed a defect in cell polarization. Transmission images show the morphology of the corresponding cell (transmission). Scale bar equals 10 μm; n = 3.

cells with respect to cell polarization, lamellipodium formation, and enrichment of Syk at the leading edge.

### Redistribution of Syk was dependent on $\beta_2$ integrin (CD11/CD18)–mediated adhesion

Next, we addressed the question whether the redistribution of Syk depended on $\beta_2$ integrin (CD11/CD18)–mediated adhesion. Therefore, the experiments were performed in the presence of immobilized fibronectin. We found that the redistribution of Syk was almost absent in fMLP-stimulated EGFP-Syk wild-type transfectants exposed to fibronectin (Figure 1B), suggesting that the redistribution was dependent on $\beta_2$ integrin–mediated adhesion. The quantitative analysis confirmed that the majority of the EGFP-Syk transfectants showed a homogenous distribution of EGFP-Syk upon exposure to fibronectin (Figure S1, available at the *Blood* website; see the Supplemental Materials link at the top of the online article). In order to study whether the redistribution of Syk required fMLP signaling, we induced adhesion by addition of $Mn^{2+}$, which is well known to allow $\beta_2$ integrin–mediated adhesion and signaling in the absence of an proinflammatory mediator (Figure 1C). We found that the dHL-60 cells underwent a shape change and showed a polarized phenotype that was associated with an enrichment of Syk at the leading edge, demonstrating that the $\beta_2$ integrin engagement was sufficient for the redistribution of Syk. In contrast, application of TNFα, a cytokine that does not induce migration, resulted in strong cell spreading and thereby interfered with cell polarization. To further confirm the finding that $\beta_2$ integrin engagement was required for the observed redistribution of Syk to the leading edge, adhesion experiments were performed using $CD18^{-/-}$ murine PMNs and $CD18^{+/+}$ PMNs for control (Figure 1D). Whereas the wild-type PMNs polarized and showed an enrichment of Syk at the leading edge upon exposure to immobilized fibrinogen, the $CD18^{-/-}$-deficient PMNs remained spherical and showed a homogenous distribution of Syk within the cell. These findings show that $\beta_2$ integrin–mediated adhesion was not only required but also sufficient for cell polarization and redistribution of Syk to the leading edge.

### Localization of Syk and Vav at the leading edge

To study the potential role of the guanine exchange factor Vav, a downstream target of Syk,[21] in the $\beta_2$ integrin–mediated Syk signaling pathway, we generated different EGFP-tagged Syk mutants (Figure 2A) and analyzed the subcellular localization of Syk and Vav in these cells. In dHL60 cells transiently transfected with the EGFP-Syk wild-type construct, Syk and Vav were enriched at the leading edge of the polarized cell (Figure 2B). This asymmetric distribution of Syk and Vav within the polarized cell was abrogated in transfectants expressing a kinase-dead mutant of Syk (EGFP-Syk K402R). Moreover, these cells were characterized by the formation of excessive lamellipodia when compared with EGFP-Syk wild-type transfectants. Similarly, the transfectants expressing the Syk construct lacking the binding site for Vav (EGFP-Syk Y348F) showed an impaired enrichment of both Syk and Vav at the leading edge and formed multiple lamellipodia. These findings suggest that the redistribution of Syk (and Vav) may be critical for ordered cell polarization. The quantitative analysis of the Syk redistribution in the transfectants is shown in Figure S1.

In order to confirm the finding that not only the redistribution of Syk but also the translocation of Vav to the leading edge depended on active Syk, we studied the distribution of Syk and Vav in polarized dHL-60 cells upon pharmacologic inhibition of Syk by piceatannol and found that the inhibition of Syk impaired the enrichment of both Syk and Vav at the leading edge (Figure S2). However, treatment of the dHL-60 cells with the Src-family kinase inhibitor PP2 did not affect the enrichment of Syk at the leading edge or its colocalization with Vav, suggesting that Src kinase activity may not be necessary for the observed redistribution of Syk and Vav (Figure S3).

Next, we generated a stable Syk-siRNA–expressing HL-60 cell clone by retroviral gene transfer. Western blot analysis demonstrated a down-regulation of Syk protein expression in the HL-60 Syk-siRNA clone to 38% compared with the expression level in control cells (100%; Figure 2C). The functional analysis revealed that the down-regulation of Syk in the Syk-siRNA clone interfered with the proper establishment of cell polarity and led to the

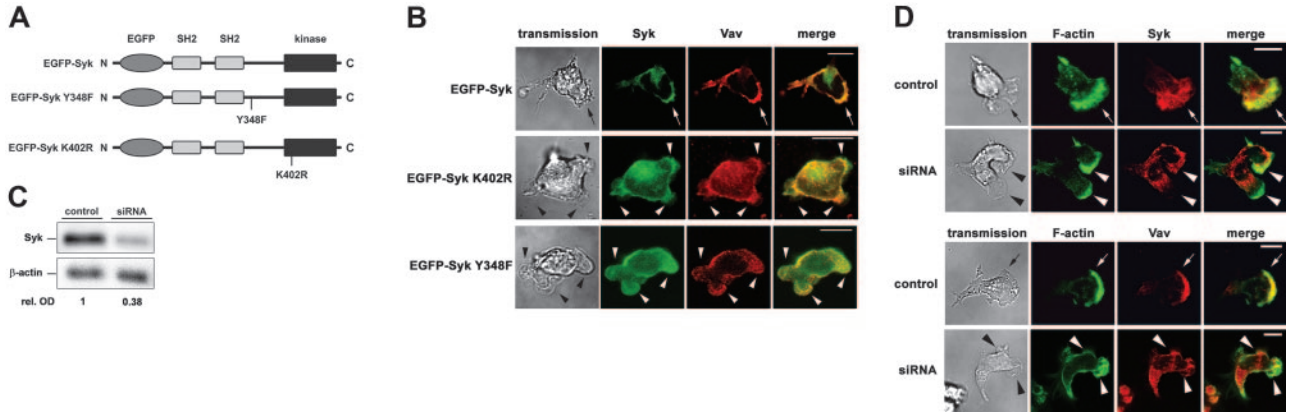


**Figure 2. Expression of Syk mutants or the down-regulation of Syk by RNAi technique compromised the enrichment of Syk and Vav at the leading edge and resulted in the formation of multiple lamellipodia.** Confocal microscopy images of human Syk detected by Syk-EGFP epifluorescence (green) or a mouse anti–human Syk mAb and a secondary Alexa 546–conjugated anti–mouse IgG Ab (red). F-actin was assessed using Alexa 488–conjugated phalloidin (green). Vav was detected using a rabbit anti-Vav Ab and a secondary Alexa 546–conjugated anti–rabbit IgG Ab (red). (A) Schematics of the Syk constructs. (B) Upon induction of adhesion by fMLP (100 nM) on immobilized fibrinogen, Syk and Vav were enriched at the leading edge (arrow) of EGFP-Syk transfectants. The merged images demonstrate colocalization (yellow). In contrast, EGFP-Syk K402R and EGFP-Syk Y348F transfectants showed no enrichment of Syk and Vav at the leading edge (arrowheads). (C) Western blot analysis of a Syk-siRNA clone (siRNA) and wild-type HL-60 cells (control) using an anti-Syk mAb and an anti–β-actin antibody for control. Numbers indicate relative optical density (OD) of Syk protein expression. (D) Upon induction of adhesion by fMLP (100 nM) on immobilized fibrinogen, the down-regulation of Syk resulted in the formation of multiple lamellipodia (arrowheads) and abolished the redistribution of Syk and Vav at the leading edge as seen in control cells. Transmission images show the morphology of the corresponding cell (transmission). Scale bar equals 10 μm; n = 3.

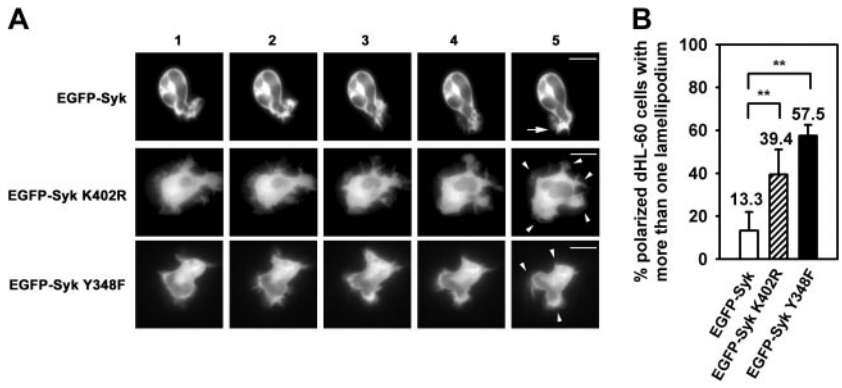


**Figure 3. Spatial and temporal instability of the leading edge in Syk mutants.** (A) Microscopic images of dHL-60 cells transiently transfected with EGFP-Syk, EGFP-Syk K402R, or EGFP-Syk Y348F constructs. Adhesion and polarization on immobilized fibrinogen was stimulated by fMLP (100 nM). Time-lapse video microscopy of the transfectants. Images were recorded at intervals of 30 seconds. EGFP-Syk was enriched at the leading edge (arrow). In contrast, EGFP-Syk K402R and EGFP-Syk Y348F transfectants showed a homogenous distribution of Syk and formed multiple lamellipodia (arrowheads). Scale bar equals 10 μm. The series shown are representative of 3 independent experiments. (B) Quantitative analysis of polarized dHL-60 cells that formed more than 1 lamellipodium upon fMLP stimulation. n = 96 (EGFP-Syk); n = 113 (EGFP-Syk K402R); n = 56 (EGFP-Syk Y348F). Counted cells were taken from at least 3 independent experiments. Means ± SD are shown. NS indicates not significant; $^{**}P < .002$.

formation of multiple lamellipodia upon stimulation by 100 nM fMLP on immobilized fibrinogen (Figure 2D). Moreover, the Syk-siRNA–expressing cells were characterized by the lack of redistribution of the remaining Syk protein as well as by the absence of Vav translocation to the leading edge, suggesting that a certain threshold of active Syk was required for the observed asymmetric distribution of these 2 signaling components within the cell and the establishment and/or maintenance of proper cell polarization.

### Spatial and temporal instability of the leading edge in Syk mutants

In order to further unravel the functional relevance of the redistribution of Syk and Vav, we analyzed the ability of the different Syk transfectants to establish and maintain a bipolar phenotype upon fMLP-mediated induction of adhesion to immobilized fibrinogen by time-lapse video microscopy in living cells (Figure 3A). The dHL60 cells expressing the EGFP-Syk wild-type construct underwent a shape change and preferentially formed one lamellipodium that was characterized by the enrichment of Syk. In contrast, the EGFP-Syk K402R kinase-dead transfectants showed multiple and unstable lamellipodia and a homogeneous distribution of Syk within the cell. This lack of the redistribution of Syk as well as the temporal and spatial instability of the leading edge was also observed in EGFP-Syk Y348F transfectants lacking the binding site for Vav. The quantitative analysis by counting polarized dHL-60 cells with more than one lamellipodium confirmed that most of the EGFP-Syk wild-type transfectants showed a proper formation of the bipolar phenotype, whereas only 13.3% formed more than one lamellipodium upon fMLP-mediated induction of adhesion to immobilized fibrinogen (Figure 3B). In contrast, the percentage of cells showing multiple lamellipodia was significantly increased to 39.4% in the EGFP-Syk K402R transfectants and to 57.5% in the EGFP-Syk Y348F transfectants, demonstrating that the kinase activity of Syk as well as its Vav binding site was important for the stabilization of the leading edge.

### Migration defect in Syk mutants and Syk-deficient murine PMNs

As the establishment of ordered cell polarity is thought to be critical for site-directed migration, we analyzed the migratory capacity of the transfectants in the presence of a chemotactic gradient (10 nM fMLP) using time-lapse video microscopy upon exposure of the cells to immobilized fibrinogen (Figure 4A). Under these experimental conditions, migration was dependent on $\beta_2$ integrin–mediated adhesion as demonstrated by the fact that migration was almost absent in $CD18^{-/-}$ PMNs (Figure S4). Using this assay, the EGFP-Syk wild-type transfectants showed a typical migratory phenotype associated with an enrichment of Syk at the lamellipodium. However, 16.0% of the cells that underwent a shape change and adhered to immobilized fibrinogen did not migrate in response to the chemoattractant (Figure 4B). The ability of the EGFP-Syk K402R transfectants to follow a chemotactic gradient was significantly impaired when compared with the EGFP-Syk wild-type transfectants. Here, 65.3% of the cells were unable to follow a chemotactic gradient. This effect was even more pronounced in the dHL-60 cells expressing the EGFP-SykY348F construct, where 83.1% of the cells did not migrate. Thus, the

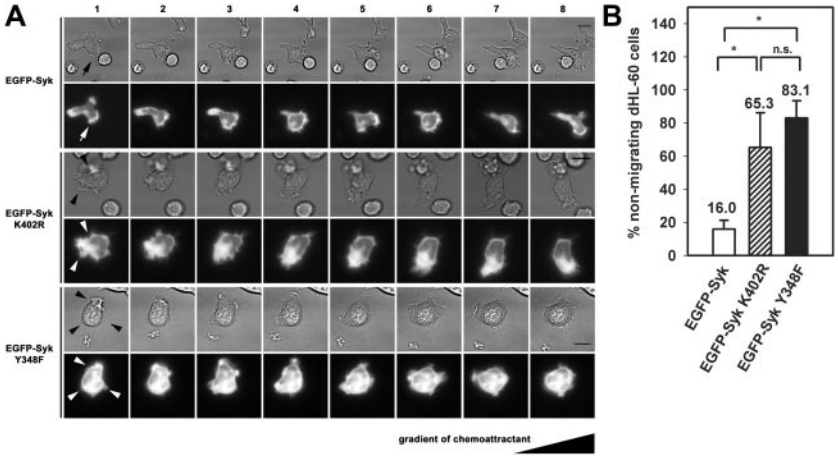


**Figure 4. Syk played a role in migration by stabilizing the leading edge.** (A) Time-lapse microscopy of dHL-60 cells transiently transfected with EGFP-Syk, EGFP-Syk K402R, or EGFP-Syk Y348F constructs. Migration on immobilized fibrinogen in response to a gradient of 10 nM fMLP is shown. Images 1 through 8 were recorded at intervals of 30 seconds. EGFP-Syk was enriched at the leading edge of the migrating cell during the observed time period (arrow). In contrast, EGFP-Syk K402R or EGFP-Syk Y348F showed a homogenous distribution within the cell. Both mutants showed multiple unstable lamellipodia and impaired migration (arrowheads). Scale bar equals 10 μm. The series shown are representative for 3 independent experiments. Supplementary video sequences show migrating EGFP-Syk wild-type (Video S1), EGFP-Syk Y348F (Video S2), and EGFP-Syk K402R transfectants (Video S3). (B) Quantitative analysis of nonmigrating dHL-60 cells. Cells were defined as nonmigrating when there was no detectable movement of the uropod during the observed time period of at least 7 minutes. n = 29 (EGFP-Syk); n = 28 (EGFP-Syk K402R); n = 27 (EGFP-Syk Y348F). Analyzed cells were taken from 3 independent experiments. Means ± SD are shown. n.s. indicates not significant; $^{*}P < .02$.

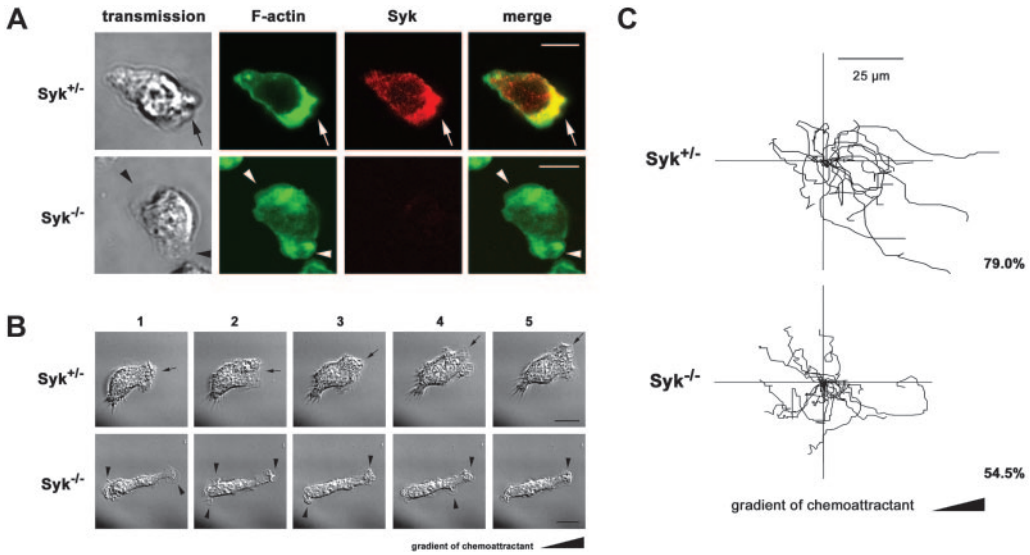


**Figure 5. Murine Syk$^{-/-}$ PMNs formed multiple lamellipodia and showed impaired site-directed migration.** (A) Confocal microscopy images of polarized murine Syk$^{+/-}$ and Syk$^{-/-}$ PMNs. Adhesion and polarization on immobilized fibrinogen was induced by fMLP (100 nM) for 30 minutes at 37°C. Indirect fluorescence staining of Syk using a polyclonal Syk Ab and a secondary Alexa 546–conjugated anti–rabbit IgG Ab (red). F-actin was assessed using Alexa 488–conjugated phalloidin (green). In Syk$^{+/-}$ cells, F-actin and Syk were enriched at the leading edge (arrow); colocalization is shown in yellow (merge). In contrast, Syk$^{-/-}$ PMNs formed multiple lamellipoda (arrowheads). Transmission images show the morphology of the corresponding cell (transmission). Scale bar equals 10 μm. (B-C) Analysis of migrating Syk$^{+/-}$ and Syk$^{-/-}$ PMNs in Zigmond chambers on immobilized fibrinogen in response to a gradient of 10 μM fMLP. (B) Time-lapse images (1-5) of Syk$^{+/-}$ and Syk$^{-/-}$ PMNs were recorded at intervals of 1 minute. Syk$^{+/-}$ PMNs formed 1 stable lamellipodium and performed site-directed migration over the observed time period (arrow). In contrast, Syk$^{-/-}$ PMNs showed multiple unstable lamellipodia (arrowheads) and impaired migration. Scale bar equals 10 μm. Supplementary video sequences show migrating Syk$^{+/-}$ PMNs (Video S4) and Syk$^{-/-}$ PMNs (Video S5). (C) Polar plot of tracked migration paths of Syk$^{+/-}$ and Syk$^{-/-}$ PMNs. Time-lapse images were taken every 15 seconds over a period of 12 minutes. In contrast to control cells, Syk$^{-/-}$ PMNs showed impaired site directed migration. Scale bar equals 25 μm. Migration tracks from one experiment are shown. Numbers indicate the percentage of cells that ended up within a 180° angle facing the source of the chemoattractant. Results are representative of 3 independent experiments.

inability of both Syk mutants to redistribute Syk and Vav to the lamellipodium not only interfered with ordered cell polarization, but also impaired the migratory capacity of the cells, suggesting a critical role for Syk and Vav in leukocyte migration. Time-lapse video microscopy of migrating EGFP-Syk wild-type–, EGFP-Syk Y348F–, and EGFP-Syk K402R–expressing dHL-60 cells is depicted in video sequences (Videos S1-S3).

To elaborate the relevance of Syk in the control of lamellipodium formation and chemotaxis, we analyzed cell polarization and migration of murine Syk$^{-/-}$ and Syk$^{+/-}$ PMNs. Upon stimulation, murine Syk$^{+/-}$ PMNs polarized on immobilized fibrinogen and redistributed Syk to the leading edge (Figure 5A). In contrast, Syk$^{-/-}$ PMNs formed multiple lamellipodia, confirming a functional role of Syk for the stabilization of cell polarity. Similar results were obtained by time-lapse video microscopy of chemotaxis in Zigmond chambers (Figure 5B). Here, Syk$^{-/-}$ PMNs were characterized by a spatial and temporal instability of cell polarization, whereas the Syk$^{+/-}$ PMNs maintained a bipolar phenotype and migrated during the observed time period (Videos S4-S5). Statistical analysis revealed that 80.5% ± 4% of the Syk$^{+/-}$ PMNs migrated compared with 32.7% ± 13% of Syk$^{-/-}$ PMNs ($P < .004$; n = 3). Next, chemotaxis was measured by counting the number of migrating cells that ended up within the 180° angle, facing the source of the chemoattractant. Figure 5C shows the original migration tracks of one representative experiment. The analysis showed that 79.0% of migrating Syk$^{+/-}$ PMNs performed chemotactic migration. In contrast, this percentage was decreased to 54.5% in migrating Syk$^{-/-}$ PMNs, which reflects nearly random migration, where theoretically 50% of the cells end up within the 180° angle. Thus, the absence of Syk down-regulated the migratory capacity of the PMNs and decreased their ability to follow a chemotactic gradient.

### A role for Syk in the acute inflammatory response

To study the role of Syk in the control of PMN activation and migration in vivo, we used the reverse-passive Arthus reaction in the ear (Figure 6). The histologic analysis of the ears of Syk$^{+/-}$ chimeric mice 6 hours after the induction of the inflammatory response revealed a robust PMN infiltration. In contrast, the PMN accumulation in the tissue was markedly diminished in Syk$^{-/-}$ chimeric mice (142.2 ± 20.5 PMNs per high-power field vs 12.3 ± 4.4 PMNs per high-power field, respectively). In accordance, edema formation (3.6 ± 0.4 mm vs 1.2 ± 0.2 mm) as well as inflammation-mediated vessel damage (hemorrhage score of 3.1 ± 0.6 vs 0.8 ± 0.3) was markedly reduced in Syk$^{-/-}$ chimeric mice when compared with Syk$^{+/-}$ chimeric control animals. Thus, these data indicate a critical role of Syk for PMN migration and activation during this immune complex–mediated acute inflammatory response in vivo.

Next, we studied the impact of Syk on PMN extravasation in cremaster muscle venules superfused with 1 μM fMLP for 15 minutes. As shown in Figure 7, the absence of Syk significantly reduced the number of intravascularly adherent PMNs by 31% compared with Syk$^{+/-}$ chimeric control mice. Similarly, adhesion of mononuclear cells from Syk$^{-/-}$ chimeric mice was reduced by 27% compared with that of controls. The number of perivascular PMNs found after fMLP stimulation was also significantly reduced in Syk$^{-/-}$ chimeric mice by 59% compared with that in Syk$^{+/-}$ chimeric mice. In contrast, mononuclear cell recruitment into the tissue was similar between Syk$^{-/-}$ chimeric mice and Syk$^{+/-}$ chimeric mice, suggesting that mononuclear cell extravasation is independent of Syk. These results indicate that Syk has functional relevance for PMN adhesion and migration in vivo, whereas infiltration of mononuclear cells into the tissue does not require Syk.

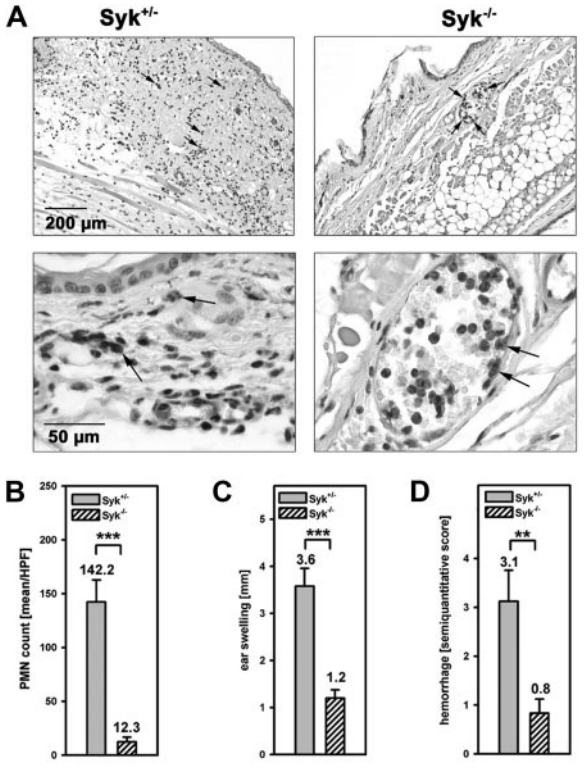


**Figure 6. A role of Syk in the acute inflammatory response.** The reverse-passive Arthus reaction was induced in the left ear of Syk$^{+/-}$ and Syk$^{-/-}$ bone marrow chimeric mice for 6 hours. (A) Gr-1 staining of PMNs (arrow) in histologic sections of the left ear. (B) PMN extravasation was determined by counting Gr-1$^+$ cells within 6 hours after treatment in 5 different microscopic fields of every section. (C) Edema formation was measured as ear swelling 6 hours after treatment. (D) Semiquantitative score for hemorrhage 6 hours after treatment. n = 4 (Syk$^{+/-}$ animals); n = 3 (Syk$^{-/-}$ animals). Means ± SD are shown. $^{**}P < .002$; $^{***}P < .001$.

## Discussion

During the acute inflammatory response, chemotaxis allows the efficient accumulation of PMNs at the sites of lesion. In the present work, we provide evidence that the non–receptor tyrosine kinase Syk is functionally involved in $\beta_2$ integrin–mediated polarization and migration of fMLP-stimulated dHL-60 cells. In this model, the kinase activity of Syk as well as its binding site for Vav at Tyr348 is required for the stabilization of the leading edge and the maintenance of cell polarity. In addition, we present in vivo data indicating a role for Syk in PMN recruitment to sites of lesion during the inflammatory response.

Cell polarization and migration were studied on immobilized fibrinogen, a well-known ligand of the $\beta_2$ integrins Mac-1 and glycoprotein (gp) 150/95 (CD11c/CD18).[18] $\beta_2$ integrin–mediated adhesion is known to cause clustering of the $\beta_2$ integrins that induces the activation of Syk.[7,8] Here, we provide evidence that $\beta_2$ integrin–mediated ligand interactions are required and sufficient for the observed redistribution of Syk in migrating PMNs. This redistribution seemed to be independent of Src-family kinases because treatment of the cells with the specific Src-family kinase inhibitor PP2 had no effect. Moreover, we demonstrated a colocalization of Syk and Vav at the leading edge of polarized dHL-60 cells that adhered to immobilized fibrinogen. The analysis of the Vav distribution revealed that the kinase activity of Syk as well as its Vav binding site is required for redistribution of both proteins to the leading edge of the polarized cell. Accordingly, Deckert et al have demonstrated that the catalytic activity of Syk and its Vav binding site are critical for efficient Vav binding in transiently transfected COS cells.[21] Furthermore, it has been demonstrated that phosphorylation of Vav at tyrosine 174, which is critical for Vav activation, is mediated by Syk, and that the expression of the Syk kinase-dead mutant completely blocks Vav phosphorylation and activation in CHO cells.[21,33,34] In the present study, we demonstrated that both the Syk K402R kinase-dead transfectants as well as the Syk Y348F transfectants lacking the binding site for Vav formed multiple and unstable lamellipodia, suggesting that the Syk-mediated control of lamellipodium formation may be due to activation of Vav. In accordance, Vav activation has been shown to occur upon $\beta_2$ integrin–mediated adhesion of murine PMNs.[35] However, Vav is also known to be critical for the control of phospholipase C$\gamma$, especially in hematopoietic cells.[22] Therefore, we cannot exclude that $\beta_2$ integrin–mediated Syk signaling affects the activity of phospholipase C$\gamma$ in our system.

Polarization of leukocytes is the morphologic equivalent of intracellular processes leading to an asymmetric distribution of signaling components. The result of this process is a persistent sensitivity for chemoattractants at the front of the cell that induces directional signaling within the cell and allows site-directed migration.[3] Thus, the observed redistribution of Syk and Vav to the front of the cell may reflect the establishment of polarized sensitivity. Accordingly, in human lymphocytes and murine macrophages, dominant-negative Vav has been reported to inhibit migration.[24,25] In contrast, studies in the murine system using Vav-1/Vav-3 double-knockout mice revealed that Vav-1/Vav-3 is not essential for PMN migration in mice.[35] These striking differences may be due to the constitutive absence of the signaling components in the knockout animals, which may lead to compensatory effects. Moreover, the molecular mechanism of leukocyte polarization and migration may differ in both species to some extent, which may explain the differences observed in both models. In the human system, Syk, Vav, and Cdc42 have been shown to become activated upon $\beta_2$ integrin–mediated adhesion.[7,36,37] Thus, our results may show that this activation is important for the stabilization of the leading edge in polarized human leukocytes, which is known to

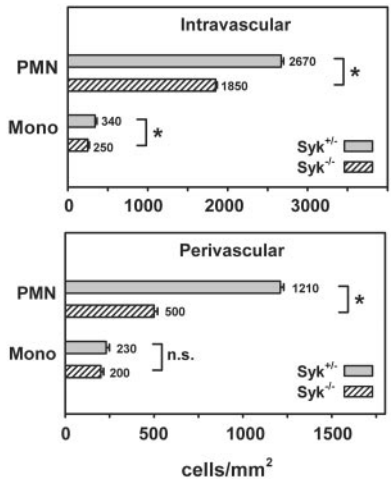


**Figure 7. Impaired PMN adhesion and extravasation in the absence of Syk.** Number of adherent leukocytes per square millimeter of venular surface area (top panel, intravascular) and perivascular leukocyte accumulation (bottom panel, perivascular) after 15 minutes of fMLP superfusion of the cremaster muscle using Syk$^{+/-}$ and Syk$^{-/-}$ bone marrow chimeric mice. Data shown represent intravascular and perivascular PMNs and mononuclear (Mono) cell counts in whole-mount preparation of the cremaster muscle. n = 4 (Syk$^{+/-}$ animals); n = 4 (Syk$^{-/-}$ animals). Means ± SEM are shown. n.s. indicates not significant; $^{*}P < .05$.

represent an essential prerequisite for chemotaxis. Accordingly, the analysis of chemotaxis by single-cell tracking revealed a migration defect in the Syk mutants and in murine $Syk^{-/-}$ PMNs. Similar results were obtained by studying migration of $Syk^{-/-}$ PMNs in the Boyden chamber at a submaximal effective dose of fMLP, whereas supraphysiologic concentrations of the chemoattractant ($> 1$ μM) induced Syk-independent migration,[38] which may show that the requirement for Syk depends on the experimental setting and the concentration of the chemoattractant used. Under the experimental conditions in the present study, PMN migration strongly depends on $\beta_2$ integrins, and thereby reflects an inflammatory situation in vivo where PMNs migrate on fibrin within the inflamed interstitial space. In contrast, the Boyden chamber assay is a rather undefined setting with respect to the requirement for different adhesion receptors. Therefore, additional mechanisms may compensate for the absence of Syk in this assay, which may explain that $Syk^{-/-}$ PMNs migrate in response to high concentrations of a chemoattractant in the Boyden chamber assay.

However, we now present in vivo evidence for an essential role of Syk by a genetic approach. Using the reverse-passive Arthus reaction as a model of an acute inflammatory response, we demonstrate that Syk was indispensable for PMN accumulation in the tissue. The Arthus reaction was induced by immune complexes, leading to the activation of the complement cascade and the consecutive generation of the bioactive complement component C5a that attracts PMNs.[39] In parallel, the immune complexes bind to Fcγ receptors on resident effector cells in the tissue.[40] As Fcγ receptors signal via Syk,[12] the striking absence on a robust inflammatory response in $Syk^{-/-}$ bone marrow chimeras may be due in part to the impaired activation of resident macrophages and mast cells. However, the activation of the complement cascade by immune complexes is independent of cellular activation. Thus, it is reasonable to speculate that the lack of PMN infiltration in the $Syk^{-/-}$ bone marrow chimeras was at least in part caused by a migration defect of PMNs in the absence of Syk. This view was confirmed by studying PMN adhesion and migration in the inflamed cremaster model upon direct activation of PMNs by superfusion of fMLP. The delineation of the requirement of Syk for the different steps of the extravasation process revealed that Syk was necessary for firm adhesion and extravasation of PMNs in vivo, whereas monocyte infiltration was independent of Syk. The robust attenuation of PMN infiltration and the striking decrease of inflammation-mediated tissue damage in the absence of Syk may imply that the inhibition of Syk represents an attractive new concept for therapeutic intervention in patients with acute inflammatory diseases.

## Acknowledgments

The expert technical assistance of Mrs S. Weidner is acknowledged. We thank Drs H. Bourne and F. Wang (University of California, San Francisco) for their help with the transient transfection of dHL-60 cells.

This work was supported by Deutsche Forschungsgemeinschaft grants DFG Wa 1048/2-1 (B.W.), SFB 497/TP C7 (K.S.-K.), and DFG 621/3-1 (M.S.).

## Authorship

J.S. collected data, analyzed data, performed research, and wrote the paper; A.S. collected data (Arthus reaction); D.F. collected data (cremaster model); M.S. performed research and analyzed data (cremaster model); R.G. contributed analytical tools (siRNA transfectants); C.T. collected data; A.M. contributed analytical tools (Syk-deficient bone marrow chimeras); K.S.-K. performed research (Arthus reaction); and B.W. designed research, analyzed the data, and wrote the paper.

The authors declare no competing financial interests.

Correspondence: Barbara Walzog, Department of Physiology, Ludwig-Maximilians-Universität München, Schillerstr. 44, D-80336 München, Germany; e-mail: walzog@lrz.uni-muenchen.de.

## References

1. Muller WA. Leukocyte-endothelial-cell interactions in leukocyte transmigration and the inflammatory response. Trends Immunol. 2003;24:327-334.
2. Moser B, Wolf M, Walz A, Loetscher P. Chemokines: multiple levels of leukocyte migration control. Trends Immunol. 2004;25:75-84.
3. Van Haastert PJ, Devreotes PN. Chemotaxis: signalling the way forward. Nat Rev Mol Cell Biol. 2004;5:626-634.
4. Li Z, Hannigan M, Mo Z, et al. Directional sensing requires Gβγ-mediated PAK1 and PIXα-dependent activation of Cdc42. Cell. 2003;114:215-227.
5. Kinashi T. Intracellular signalling controlling integrin activation in lymphocytes. Nat Rev Immunol. 2005;5:546-559.
6. Anderson DC, Springer TA. Leukocyte adhesion deficiency: an inherited defect in the Mac-1, LFA-1, and p150,95 glycoproteins. Annu Rev Med. 1987;38:174-195.
7. Willeke T, Schymeinsky J, Prange P, Zahler S, Walzog B. A role for Syk-kinase in the control of the binding cycle of the $\beta_2$ integrins (CD11/CD18) in human polymorphonuclear neutrophils. J Leukoc Biol. 2003;74:260-269.
8. Yan SR, Huang M, Berton G. Signaling by adhesion in human neutrophils: activation of the p72syk tyrosine kinase and formation of protein complexes containing p72syk and Src family kinases in neutrophils spreading over fibrinogen. J Immunol. 1997;158:1902-1910.
9. Miura Y, Tohyama Y, Hishita T, et al. Pyk2 and Syk participate in functional activation of granulocytic HL-60 cells in a different manner. Blood. 2000;96:1733-1739.
10. Kiefer F, Brumell J, Al-Alawi N, et al. The Syk protein tyrosine kinase is essential for Fcγ receptor signaling in macrophages and neutrophils. Mol Cell Biol. 1998;18:4209-4220.
11. Minami Y, Nakagawa Y, Kawahara A, et al. Protein tyrosine kinase Syk is associated with and activated by the IL-2 receptor: possible link with the c-myc induction pathway. Immunity. 1995;2:89-100.
12. Berton G, Mocsai A, Lowell CA. Src and Syk kinases: key regulators of phagocytic cell activation. Trends Immunol. 2005;26:208-214.
13. Cheng AM, Rowley B, Pao W, Hayday A, Bolen JB, Pawson T. Syk tyrosine kinase required for mouse viability and B-cell development. Nature. 1995;378:303-306.
14. Turner M, Mee PJ, Costello PS, et al. Perinatal lethality and blocked B-cell development in mice lacking the tyrosine kinase Syk. Nature. 1995;378:298-302.
15. Poole A, Gibbins JM, Turner M, et al. The Fc receptor γ-chain and the tyrosine kinase Syk are essential for activation of mouse platelets by collagen. EMBO J. 1997;16:2333-2341.
16. Obergfell A, Eto K, Mocsai A, et al. Coordinate interactions of Csk, Src, and Syk kinases with αIIbβ3 initiate integrin signaling to the cytoskeleton. J Cell Biol. 2002;157:265-275.
17. Sada K, Takano T, Yanagi S, Yamura H. Structure and function of Syk protein-tyrosine kinase. J Biochem. 2001;130:177-186.
18. Plow EF, Haas TA, Zhang L, Loftus J, Smith JW. Ligand binding to integrins. J Biol Chem. 2000;275:21785-21788.
19. Mócsai A, Zhou M, Meng F, Tybulewicz VL, Lowell CA. Syk is required for integrin signaling in neutrophils. Immunity. 2002;16:547-558.
20. Schymeinsky J, Then C, Walzog B. The non-receptor tyrosine kinase Syk regulates lamellipodium formation and site-directed migration of human leukocytes. J Cell Physiol. 2005;204:614-622.
21. Deckert M, Tartare-Deckert S, Couture C, Mustelin T, Altman A. Functional and physical interactions of Syk family kinases with the Vav proto-oncogene product. Immunity. 1996;5:591-604.
22. Turner M, Billadeau DD. VAV proteins as signal integrators for multi-subunit immune-recognition receptors. Nat Rev Immunol. 2002;2:476-486.
23. Srinivasan S, Wang F, Glavas S, et al. Rac and Cdc42 play distinct roles in regulating PI(3,4,5)P3 and polarity during neutrophil chemotaxis. J Cell Biol. 2003;160:375-385.

24. Vicente-Manzanares M, Cruz-Adalia A, Martin-Cofreces NB, et al. Control of lymphocyte shape and the chemotactic response by the GTP exchange factor Vav. Blood. 2005;105:3026-3034.
25. Vedham V, Phee H, Coggeshall KM. Vav activation and function as a rac guanine nucleotide exchange factor in macrophage colony-stimulating factor-induced macrophage chemotaxis. Mol Cell Biol. 2005;25:4211-4220.
26. Scharffetter-Kochanek K, Lu H, Norman K, et al. Spontaneous skin ulceration and defective T cell function in CD18 null mice. J Exp Med. 1998;188:119-131.
27. Takada Y, Aggarwal BB. TNF activates Syk protein tyrosine kinase leading to TNF-induced MAPK activation, NF-κB activation, and apoptosis. J Immunol. 2004;173:1066-1077.
28. Ory DS, Neugeboren BA, Mulligan RC. A stable human-derived packaging cell line for production of high titer retrovirus/vesicular stomatitis virus G pseudotypes. Proc Natl Acad Sci U S A. 1996;93:11400-11406.
29. Zigmond SH. Ability of polymorphonuclear leukocytes to orient in gradients of chemotactic factors. J Cell Biol. 1977;75:606-616.
30. Sunderkotter C, Seeliger S, Schonlau F, et al. Different pathways leading to cutaneous leukocytoclastic vasculitis in mice. Exp Dermatol. 2001;10:391-404.
31. Peters T, Sindrilaru A, Hinz B, et al. Wound-healing defect of $CD18^{-/-}$ mice due to a decrease in TGF-$\beta_1$ and myofibroblast differentiation. EMBO J. 2005;24:3400-3410.
32. Sperandio M, Thatte A, Foy D, et al. Severe impairment of leukocyte rolling in venules of core 2 glucosaminyltransferase-deficient mice. Blood. 2001;97:3812-3819.
33. Miranti CK, Leng L, Maschberger P, Brugge JS, Shattil SJ. Identification of a novel integrin signaling pathway involving the kinase Syk and the guanine nucleotide exchange factor Vav1. Curr Biol. 1998;8:1289-1299.
34. López-Lago M, Lee H, Cruz C, Movilla N, Bustelo XR. Tyrosine phosphorylation mediates both activation and downmodulation of the biological activity of Vav. Mol Cell Biol. 2000;20:1678-1691.
35. Gakidis MA, Cullere X, Olson T, et al. Vav GEFs are required for $\beta_2$ integrin-dependent functions of neutrophils. J Cell Biol. 2004;166:273-282.
36. Zheng L, Sjolander A, Eckerdal J, Andersson T. Antibody-induced engagement of $\beta_2$ integrins on adherent human neutrophils triggers activation of p21ras through tyrosine phosphorylation of the protooncogene product Vav. Proc Natl Acad Sci U S A. 1996;93:8431-8436.
37. Dib K, Melander F, Axelsson L, Dagher MC, Aspenstrom P, Andersson T. Down-regulation of Rac activity during $\beta_2$ integrin-mediated adhesion of human neutrophils. J Biol Chem. 2003;278:24181-24188.
38. Mócsai A, Zhang H, Jakus Z, Kitaura J, Kawakami T, Lowell CA. G-protein-coupled receptor signaling in Syk-deficient neutrophils and mast cells. Blood. 2003;101:4155-4163.
39. Marder SR, Chenoweth DE, Goldstein IM, Perez HD. Chemotactic responses of human peripheral blood monocytes to the complement-derived peptides C5a and C5a des Arg. J Immunol. 1985;134:3325-3331.
40. Baumann U, Kohl J, Tschernig T, et al. A codominant role of Fc-γRI/III and C5aR in the reverse Arthus reaction. J Immunol. 2000;164:1065-1070.